Abscisic acid-independent stomatal CO_2 signal transduction pathway and convergence of CO_2 and ABA signaling downstream of OST1 kinase

Po-Kai Hsu[a], Yohei Takahashi[a], Shintaro Munemasa[b], Ebe Merilo[c], Kristiina Laanemets[d], Rainer Waadt[e], Dianne Pater[a], Hannes Kollist[c], and Julian I. Schroeder[a,1]

[a]Cell and Developmental Biology Section, Division of Biological Sciences, University of California, San Diego, La Jolla, CA 92093; [b]Graduate School of Environmental and Life Science, Okayama University, 7008530 Okayama, Japan; [c]Institute of Technology, University of Tartu, 50411 Tartu, Estonia; [d]Plant Biotechnology Department, Estonian Crop Research Institute, 48309 Jõgeva, Estonia; and [e]Centre for Organismal Studies, Plant Developmental Biology, University of Heidelberg, 69120 Heidelberg, Germany

Contributed by Julian I. Schroeder, August 27, 2018 (sent for review May 29, 2018; reviewed by Hillel Fromm and Jian-Kang Zhu)

Stomatal pore apertures are narrowing globally due to the continuing rise in atmospheric [CO_2]. CO_2 elevation and the plant hormone abscisic acid (ABA) both induce rapid stomatal closure. However, the underlying signal transduction mechanisms for CO_2/ABA interaction remain unclear. Two models have been considered: (*i*) CO_2 elevation enhances ABA concentrations and/or early ABA signaling in guard cells to induce stomatal closure and (*ii*) CO_2 signaling merges with ABA at OST1/SnRK2.6 protein kinase activation. Here we use genetics, ABA-reporter imaging, stomatal conductance, patch clamp, and biochemical analyses to investigate these models. The strong ABA biosynthesis mutants *nced3/nced5* and *aba2-1* remain responsive to CO_2 elevation. Rapid CO_2-triggered stomatal closure in PYR/RCAR ABA receptor quadruple and hextuple mutants is not disrupted but delayed. Time-resolved ABA concentration monitoring in guard cells using a FRET-based ABA-reporter, ABAleon2.15, and ABA reporter gene assays suggest that CO_2 elevation does not trigger [ABA] increases in guard cells, in contrast to control ABA exposures. Moreover, CO_2 activates guard cell S-type anion channels in *nced3/nced5* and ABA receptor hextuple mutants. Unexpectedly, in-gel protein kinase assays show that unlike ABA, elevated CO_2 does not activate OST1/SnRK2 kinases in guard cells. The present study points to a model in which rapid CO_2 signal transduction leading to stomatal closure occurs via an ABA-independent pathway downstream of OST1/SnRK2.6. Basal ABA signaling and OST1/SnRK2 activity are required to facilitate the stomatal response to elevated CO_2. These findings provide insights into the interaction between CO_2/ABA signal transduction in light of the continuing rise in atmospheric [CO_2].

CO_2 | ABA | stomatal closure | carbon dioxide | abscisic acid

Stomatal pores are formed by pairs of guard cells on the surfaces of leaves to control transpirational water loss and CO_2 availability for photosynthesis. Plants need to optimally regulate stomatal apertures to acclimate and survive under diverse environmental stresses. Stomatal opening is triggered by blue and red light (1), reduced CO_2 concentrations in the intercellular air spaces of leaves (2), and increased relative air humidity. Stomatal closure is triggered by abscisic acid (ABA), darkness, elevated [CO_2], and reduced relative air humidity (3, 4). Changes in stomatal aperture are controlled by changes in the concentrations of ions and osmotically active solutes in guard cells that drive osmotic water uptake or efflux from guard cells (3, 4).

ABA receptors and core signaling cascades have been identified, including PYR/RCAR ABA receptors, type 2C protein phosphatases, and SnRK2-type protein kinases (5–7). ABA-triggered stomatal closure is transduced by core ABA signal transduction components, Ca^{2+}, and reactive oxygen species (8–14). In *Arabidopsis*, ABA biosynthesis via the 9-*cis*-epoxycarotenoid dioxygenases NCED3 and NCED5, and the xanthoxin dehydrogenase ABA2, followed by downstream signaling via PYR/RCAR ABA receptors has been shown to be crucial for ABA-induced stomatal closure and drought tolerance (5, 6, 15–20).

The sensing and signal transduction mechanisms that cause elevated CO_2-induced stomatal closure remain less well understood. Molecular components, including BETA CARBONIC ANHYDRASEs (βCA1 and βCA4), HIGH LEAF TEMPERATURE1 (HT1), OPEN STOMATA 1 (OST1/SnRK2.6), SLOW ANION CHANNEL-ASSOCIATED 1 (SLAC1), ALMT12/QUAC1 anion channel, GROWTH CONTROLLED BY ABA2 (GCA2), RESISTANT TO HIGH CO_2 (RHC1), GUARD CELL HYDROGEN PEROXIDE-RESISTANT1 (GHR1), and MITOGEN-ACTIVATED PROTEIN KINASE12 (MPK12), have been identified to be involved in stomatal CO_2 signal transduction (21–30). The detailed interaction and regulation mechanisms among these components and additional key components including the unknown CO_2/HCO_3^- sensors remain to be identified.

Anion efflux from guard cells is a central control mechanism for the regulation of stomatal closure (23, 24, 31). Slow (S-type) anion channels are encoded by the *SLAC1* gene, which is a major component responsible for mediating anion efflux in *Arabidopsis* guard cells, and *slac1* mutants are impaired in ABA- and CO_2-induced stomatal closure (23, 24). The S-type anion channel

Significance

Elevated CO_2 and abscisic acid (ABA) induce rapid stomatal closure, but the underlying signal transduction mechanisms of CO_2/ABA interaction remain unclear. Here we show that elevated CO_2-induced stomatal closure is not abolished but is slowed in higher-order ABA biosynthesis and receptor mutants. Physiological CO_2 elevations activate anion channels in these mutants. In vivo time-resolved ABA nanoreporter imaging indicates that CO_2 elevation does not change ABA concentrations in guard cells. Unexpectedly, CO_2 signaling proceeds without direct OST1/SnRK2 kinase activation in guard cells. This study points to a model that elevated CO_2 triggers stomatal closure through an ABA-independent pathway downstream of OST1/SnRK2 kinases and that basal ABA signaling and OST1/SnRK2 activity enhance stomatal closure in response to CO_2 elevation.

Author contributions: P.-K.H., Y.T., and J.I.S. designed research; P.-K.H., Y.T., S.M., E.M., K.L., and D.P. performed research; R.W. contributed new reagents/analytic tools; P.-K.H., Y.T., S.M., E.M., K.L., H.K., and J.I.S. analyzed data; and P.-K.H. and J.I.S. wrote the paper.

Reviewers: H.F., Tel Aviv University; and J.-K.Z., Purdue University.

The authors declare no conflict of interest.

[1]To whom correspondence should be addressed. Email: jischroeder@ucsd.edu.

This article contains supporting information online at www.pnas.org/lookup/suppl/doi:10.1073/pnas.1809204115/-/DCSupplemental.

Published online October 3, 2018.

activity of SLAC1 in oocytes and guard cells is enhanced via phosphorylation by the Ser/Thr protein kinase OST1/SnRK2.6 (32–35). Mutants in *OST1/SnRK2.6* are strongly impaired in both ABA- and CO_2-induced stomatal closure (8, 27, 28, 36) leading to the present model that ABA and CO_2 converge upstream of or at the level of OST1/SnRK2.6 kinase activation (27, 36, 37).

Classical studies have suggested that ABA modulates elevated CO_2-induced stomatal closure and CO_2 affects ABA-induced stomatal closure in *Xanthium strumarium* (38, 39). However, the molecular, biochemical, and cellular mechanisms underlying CO_2/ABA interaction have remained enigmatic. Research has indicated that elevated CO_2-induced stomatal closure is slowed in the PYR/RCAR ABA receptor *pyr1/pyl1/pyl2/pyl4* (*rcar10/11/12/14*) quadruple mutant (27). However, it was recently reported that elevated CO_2-induced stomatal closure is completely abolished in the same ABA receptor *pyr1/pyl1/pyl2/pyl4* (*rcar10/11/12/14*) quadruple mutant and in the strong ABA biosynthesis *nced3/nced5* double mutant (37). Two possible models for early CO_2 signal transduction have been debated: (*i*) the convergence point of CO_2 and ABA signaling is located downstream of ABA synthesis and ABA receptors but upstream of or at the level of OST1/SnRK2.6 protein kinase activation and (*ii*) elevated CO_2 rapidly increases ABA concentration or ABA signal transduction in guard cells to mediate stomatal closing (see models in refs. 27, 28, 36, 37).

In this study, we used genetics, cell imaging, time-resolved intact plant and leaf stomatal conductance, patch clamp, and guard cell biochemical analyses to critically analyze present models for the function of ABA signal transduction in rapid CO_2-induced stomatal closure. We investigated stomatal CO_2 responses in ABA biosynthesis mutants and ABA receptor mutants by intact leaf and intact whole rosette gas exchange analyses. Time-resolved ABA concentration changes in guard cells in response to extracellular CO_2 elevation were directly monitored using an ABA FRET-reporter. In addition, the effects of CO_2 concentration changes and ABA on OST1/SnRK2 kinase activities were examined by in-gel protein kinase assays of guard cells. Furthermore, elevated CO_2-induced activation of S-type anion channels in guard cells by physiological CO_2 concentration changes were investigated in ABA biosynthesis and ABA receptor mutants. Taken together, these studies point to a model for the convergence of CO_2 and ABA signal transduction downstream of OST1 protein kinase activation.

Results

CO_2-Induced Stomatal Closing in ABA Biosynthesis and ABA Signal Transduction Mutants. Both elevated CO_2 and ABA trigger stomatal closure. To analyze whether ABA is required for rapid CO_2-triggered stomatal closure, stomatal CO_2 responses were investigated in intact leaves attached to plants and in intact whole plants of ABA biosynthesis mutants. Plants of the *nced3/nced5* double mutant are defective in two major genes encoding 9-*cis*-epoxycarotenoid dioxygenase required for ABA biosynthesis (18). Mutant plants of *nced3/nced5* do not show a drought-induced increase in ABA and only retain about 2% of leaf ABA content under drought conditions compared with wild type (18). However, the *nced3/nced5* mutant plants retained about 30% of rosette leaf ABA content under well-watered conditions compared with wild type (*SI Appendix*, Fig. S1). Furthermore, the *nced3/nced5* double mutant had a significantly higher stomatal index and stomatal density (*SI Appendix*, Fig. S2), which is in line with other studies (37). Consistent with the lower ABA level and higher stomatal density, the *nced3/nced5* double mutant exhibited substantially higher basal leaf stomatal conductances at 360 ppm CO_2 compared with wild type (Fig. 1*A*). In both WT and *nced3/nced5* double mutants, shifting CO_2 from 360 to 800 ppm caused rapid stomatal closure responses (Fig. 1 *A* and *B*). Stomatal conductance appeared to be transiently reduced in *nced3/nced5* upon 800 ppm CO_2 treatment showing a gradual increase in conductance at 800 ppm CO_2 (Fig. 1 *A* and *B*). To further investigate this observation, leaf stomatal conductances were measured in response to ambient 800 ppm CO_2 for an extended duration of 90 min (Fig. 1 *C* and *D*). Furthermore, we included an additional ABA biosynthesis mutant, *aba2-1*, in these experiments. Similar to *nced3/nced5* mutant leaves, the ABA content in *aba2-1* rosettes was also about 30% of that in WT rosettes. Stomatal index as well as stomatal density in *aba2-1* leaves was higher than in WT leaves (*SI Appendix*, Figs. S1 and S2), consistent with previous studies (37, 40). WT leaves maintained low stomatal conductances after 90 min of 800 ppm CO_2 exposure (Fig. 1 *C* and *D*). However, the rapid CO_2-induced reduction in stomatal conductances in both *nced3/nced5* and *aba2-1* leaves reached minimum stomatal conductances at ∼10–16 min after shifts to 800 ppm CO_2, and then the stomatal conductance started to increase gradually but did not reach the level at 360 ppm CO_2 (Fig. 1 *C* and *D*). The absolute reductions in stomatal conductance were analyzed at 10 and 70 min after the 800 ppm CO_2 transition (Fig. 1 *E* and *F*). The three tested genotypes all showed a rapid and a continued reduction in stomatal conductance in response to CO_2 elevation (Fig. 1 *E* and *F*). However, the absolute responses after 70 min in *nced3/nced5* and *aba2-1* mutants were attenuated compared with wild type (Fig. 1*F*).

The CO_2 responses in the *nced3/nced5* double mutant and another *ABA2* null mutant, *aba2-11* (41), were also investigated by intact whole-plant (rosette) time-resolved stomatal conductance gas exchange analyses. The results again showed that *nced3/nced5* and *aba2-11* mutants retained their ability to respond rapidly to CO_2 concentration elevation (*SI Appendix*, Fig. S3). These data suggest that ABA biosynthesis mutants do not disrupt the rapid response to CO_2 elevation but can affect the long-term response to CO_2.

To further test if CO_2 triggers stomatal closure through ABA signaling, the stomatal CO_2 response was examined in PYR/RCAR ABA receptor mutants that impair ABA signaling in guard cells (19). Stomatal CO_2 responses were initially analyzed in intact leaves of ABA receptor quadruple mutant plants, *pyr1/pyl1/pyl2/pyl4* (*rcar10/11/12/14*) and *pyr1/pyl4/pyl5/pyl8* (*rcar3/8/10/11*) (Fig. 2). CO_2-triggered stomatal closure was delayed in *pyr1/pyl1/pyl2/pyl4* quadruple mutant (Fig. 2 *A* and *B*). These findings are consistent with previous observations (27) but lie in contrast to recent observations indicating complete disruption of the CO_2 response in the *pyr1/pyl1/pyl2/pyl4* quadruple mutant (37). In a different *pyr1/pyl4/pyl5/pyl8* quadruple mutant, the CO_2 response kinetics were comparable to wild type (Fig. 2*C*). However, the normalized stomatal conductance showed a reduced CO_2 response in *pyr1/pyl4/pyl5/pyl8* quadruple mutant leaves (Fig. 2*D*).

The changes in stomatal conductance at 10 and 40 min after shifting [CO_2] from 360 to 800 ppm and the half-response times were analyzed to quantify the magnitude and the rate of the stomatal CO_2 responses in these genotypes. No significant differences in the absolute shifts in stomatal conductance and the half-response times were found between *pyr1/pyl4/pyl5/pyl8* and wild type (Fig. 2 *E–G*; $P = 0.99$ in Fig. 2*E*, $P = 0.30$ in Fig. 2*F*, and $P = 0.84$ in Fig. 2*G*; one-way ANOVA followed by Dunnett's test). The absolute reduction in stomatal conductance at 40 min and the half-response time in *pyr1/pyl1/pyl2/pyl4* quadruple mutant leaves were significantly larger than in wild type (Fig. 2 *F* and *G*; $P < 0.05$ in Fig. 2*F* and $P < 0.01$ in Fig. 2*G*; one-way ANOVA followed by Dunnett's test).

Stomatal CO_2 responses were further analyzed in intact leaves of ABA receptor *pyr1/pyl2/pyl4/pyl5/pyl8* (*rcar3/8/10/11/14*) quintuple and *pyr1/pyl1/pyl2/pyl4/pyl5/pyl8* (*rcar3/8/10/11/12/14*) hextuple mutants (Fig. 3). The stomata in both *pyr1/pyl2/pyl4/pyl5/pyl8* quintuple mutant and *pyr1/pyl1/pyl2/pyl4/pyl5/pyl8* hextuple mutant leaves responded to 360 to 800 ppm CO_2 transitions, but notably, the kinetics were substantially different from WT plants

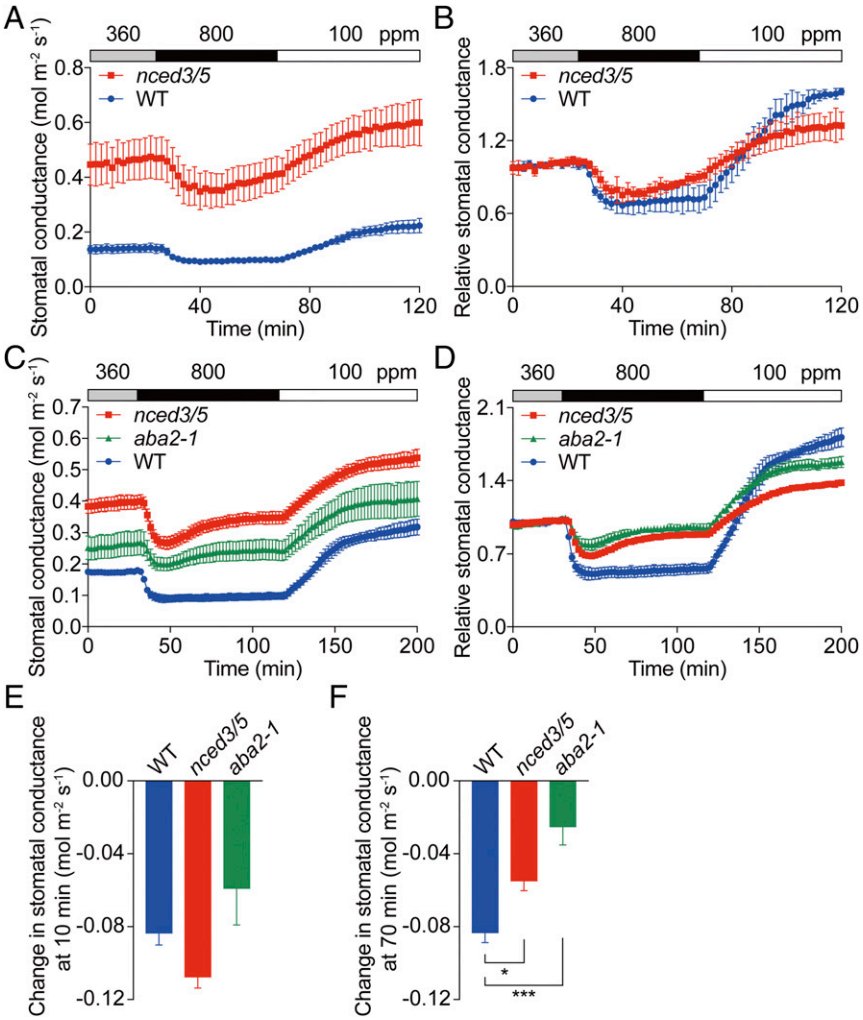

Fig. 1. Stomata of ABA biosynthesis mutants are responsive to CO_2 concentration changes. Time-resolved stomatal conductance responses to changes in [CO_2] in Col-0 (WT), *nced3/nced5* double mutant (*nced3/5*), and *aba2-1* mutant leaves. CO_2 concentrations are shown on top of the data traces in each panel. (*A*) Stomatal responses to high [CO_2] exposure for 44 min. $n = 4$ plants for each genotype. (*B*) The corresponding relative stomatal conductance responses shown in *A*. (*C*) Stomatal responses to high [CO_2] exposure for 90 min. $n = 4$ plants for WT, $n = 5$ plants for *nced3/nced5*, and $n = 4$ plants for *aba2-1*. (*D*) The corresponding relative stomatal conductance responses shown in *C*. Relative stomatal conductances were calculated by normalizing to the average stomatal conductance at 360 ppm CO_2. Absolute reduction in stomatal conductance after switching from 360 to 800 ppm CO_2 for (*E*) 10 min or (*F*) 70 min. Data represent mean ± SEM. $^*P < 0.05$, $^{***}P < 0.001$ as analyzed by one-way ANOVA followed by a Dunnett's test compared with WT control. Similar results were found in an independent set of experiments.

(Fig. 3 *A*–*D*). The normalized stomatal conductances showed a reduced elevated-CO_2 response in *pyr1/pyl2/pyl4/pyl5/pyl8* quintuple mutant leaves (Fig. 3*B*). No significant difference in the absolute change of stomatal conductance at 10 and 40 min after shifting [CO_2] from 360 to 800 ppm and the half-response time was found between *pyr1/pyl2/pyl4/pyl5/pyl8* quintuple mutant and WT leaves (Fig. 3 *E*–*G*; $P = 0.56$ in Fig. 3*E*, $P = 0.29$ in Fig. 3*F*, and $P = 0.99$ in Fig. 3*G*; one-way ANOVA followed by Dunnett's test). Control experiments showed a stable stomatal conductance at 360 ppm CO_2 in *pyr1/pyl1/pyl2/pyl4/pyl5/pyl8* hextuple mutant leaves (*SI Appendix*, Fig. S4). The absolute changes in stomatal conductance in *pyr1/pyl1/pyl2/pyl4/pyl5/pyl8* hextuple mutant leaves were much smaller than wild type at 10 min but comparable with wild type at 40 min after shifting from 360 to 800 ppm CO_2 (Fig. 3 *E* and *F*). The half-response time in *pyr1/pyl1/pyl2/pyl4/pyl5/pyl8* hextuple mutant leaves was six times slower than in WT plants (Fig. 3*G*).

The delayed elevated-CO_2 responses in *pyr1/pyl1/pyl2/pyl4* quadruple mutant (Fig. 2 *A* and *G*) and *pyr1/pyl1/pyl2/pyl4/pyl5/pyl8* hextuple mutant (Fig. 3 *C* and *G*) leaves are not only caused by the addition of the *pyl1* mutation compared with the *pyr1/pyl2/pyl4/pyl5/pyl8* quintuple mutant, because leaves of the *pyl1-1* single mutant did not exhibit any clear defect in the stomatal CO_2 response (*SI Appendix*, Fig. S5). The high basal stomatal conductances in ABA receptor mutants (Figs. 2 *A* and *C* and 3 *A* and *C*) are at least partially due to significantly higher stomatal index and stomatal density in these mutants except of the *pyr1/pyl2/pyl4/pyl5/pyl8* quintuple mutant (*SI Appendix*, Fig. S2). The OST1/SnRK2.6 protein kinase is required for ABA-induced stomatal closure (8). Stomatal conductance responses in *ost1-3* mutant leaves were investigated under the present growth conditions to further examine the involvement of ABA signal transduction in the stomatal CO_2 response. Similar to *pyr1/pyl1/pyl2/pyl4/pyl5/pyl8* hextuple mutant leaves, we found that elevated CO_2-triggered stomatal closure was substantially slowed in *ost1-3* compared with wild type under the imposed growth conditions (*SI Appendix*, Fig. S6) (27, 42). These results indicate that ABA signal transduction accelerates stomatal responses to CO_2 elevation.

The *RBOHD* and *RBOHF* genes encode two NADPH oxidases belonging to the respiratory burst oxidase homolog (RBOH) family in *Arabidopsis* (43). Double mutation of *RBOHD* and *RBOHF* impairs ABA activation of Ca^{2+}-permeable channels in guard cells and partially impairs ABA-induced stomatal closing (44). The *rbohD/rhohF* double mutant allele was recently reported to disrupt CO_2-induced stomatal closing (37). We further analyzed *rbohD/rbohF* double mutant plants to investigate whether they are required for rapid elevated CO_2-induced stomatal closure in intact leaves. Stomatal responses to elevated CO_2 in *rbohD/rbohF* double mutant leaves were similar to those in WT leaves (*SI Appendix*, Fig. S7*A*), and similar results were also independently found in intact whole-plant gas exchange analyses (*SI Appendix*, Fig. S7*B*).

Effect of CO_2 Elevation on Guard Cell ABA Concentrations. A proposed rapid rise in ABA concentration in guard cells in response to CO_2 elevation has not been directly investigated. To enable

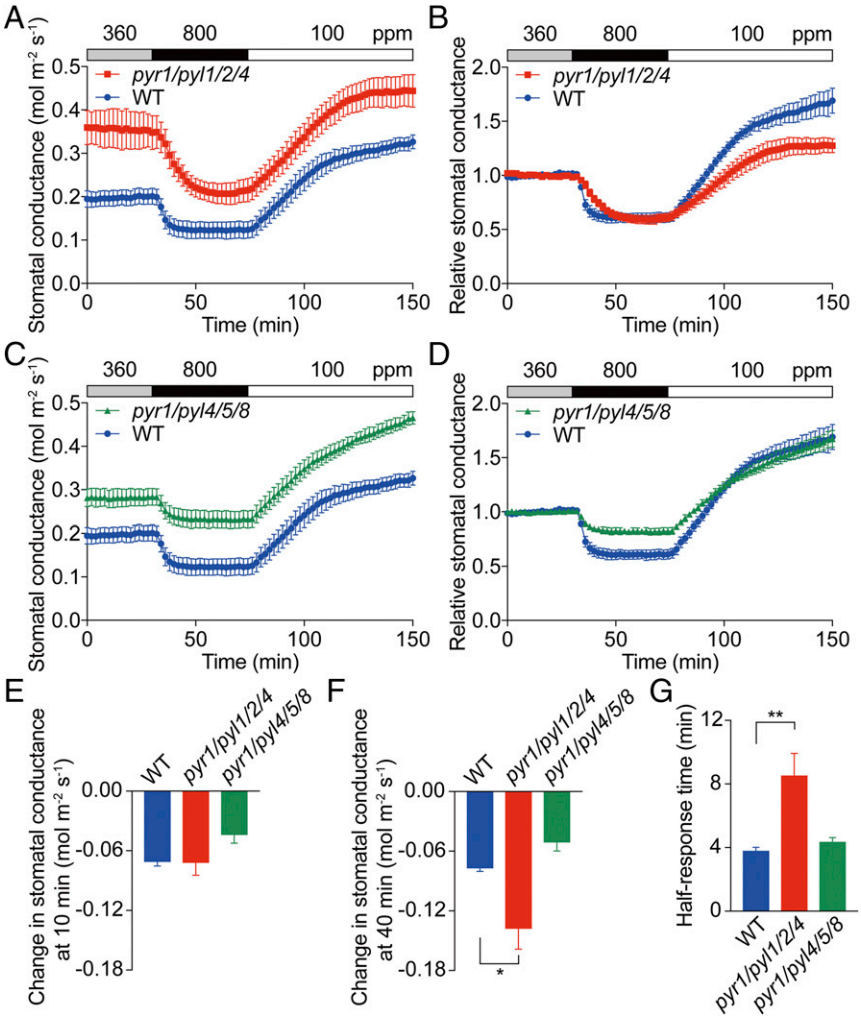

Fig. 2. Stomata of ABA receptor quadruple mutants are responsive to CO_2 concentration changes. Time-resolved stomatal conductance responses to changes in [CO_2] in Col-0 (WT), *pyr1/pyl1/pyl2/pyl4* (*rcar10/11/12/14*) quadruple mutant (*pyr1/pyl1/2/4*), and *pyr1/pyl4/pyl5/pyl8* (*rcar3/8/10/11*) quadruple mutant (*pyr1/pyl4/5/8*) leaves. CO_2 concentrations are shown on top of the data traces in each panel. (*A*) Absolute average stomatal conductances of WT and *pyr1/pyl1/2/4* quadruple mutant leaves. (*B*) The corresponding relative stomatal conductance responses shown in *A*. (*C*) Absolute average stomatal conductances of WT and *pyr1/pyl4/5/8* quadruple mutant leaves. (*D*) The corresponding relative stomatal conductance responses shown in *C*. Relative stomatal conductances were calculated by normalizing to the average stomatal conductance at 360 ppm CO_2. Note that data from WT leaves in *A* and *C* are the same because the data were obtained in the same experimental dataset. Absolute reduction in stomatal conductance after switching from 360 to 800 ppm CO_2 for (*E*) 10 min or (*F*) 40 min. (*G*) Average half-response times to 800 ppm CO_2 transition. WT controls are the same because mutants and WT were analyzed in parallel. $n = 5$ plants for each genotype in all panels. Data represent mean ± SEM. $^*P < 0.05$, $^{**}P < 0.01$ as analyzed by one-way ANOVA followed by a Dunnett's test compared with WT control. Data in *A*–*G* represent one of three sets of experiments showing similar results.

time-resolved analyses of guard cell ABA concentrations, transgenic plants expressing a fluorescence (Förster) resonance energy transfer (FRET)-based ABA reporter, ABAleon2.15 (45), driven by the guard cell preferential promoter, *pGC1* (46), were generated. Fluorescence emission ratios decrease upon binding of ABA to the ABAleon2.15 nanoreporter in plant cells (45, 47). The fluorescence emission ratios of ABAleon2.15 in guard cells were slightly reduced upon 140 mM NaCl or 20 μM ABA treatments compared with 0.02% EtOH controls (*SI Appendix*, Fig. S8*A*). In addition, low water potential of −0.76 MPa generated by PEG-8000 also slightly reduced the fluorescence emission ratios of ABAleon2.15 in guard cells compared with half-strength MS medium control with a water potential of −0.31 MPa (*SI Appendix*, Fig. S8*B*).

In control experiments, when leaf epidermes were exposed to low CO_2 buffer (115 ppm), average emission ratios of ABAleon2.15 in guard cells showed no clear change in the first 50 min followed by a slow decline (Fig. 4*A*), subsequently a rapid decrease in emission ratios was observed upon exposure to 10 μM exogenous ABA reporting an [ABA] increase in guard cells (Fig. 4*A*). Emission ratios of ABAleon2.15 in guard cells showed no clear average change in the first 30 min after shifting from low CO_2 buffer (115 ppm) to elevated CO_2 buffer (535 ppm), which was followed by a slight and slow emission ratio decline (Fig. 4*B*). Subsequent exposure to 10 μM exogenous ABA induced a rapid decrease in the ABAleon2.15 emission ratio (Fig. 4*B*), indicating that elevated CO_2 does not alter ABA concentration in guard cells in the first 15 min of CO_2 elevation when stomatal closing is largely complete (e.g., Figs. 1–3).

The long-term effect of elevated CO_2 on guard cell ABA concentrations was further investigated using an ABA-responsive promoter, *pRAB18* (48), driving green fluorescent protein (GFP) as a reporter. An enhancement of ABA signal transduction was observed in leaf abaxial epidermes of *pRAB18::GFP* transgenic plants after 9 h exposure to a lower water potential of −0.76 MPa generated by PEG-8000 compared with half-strength MS medium control with a water potential of −0.31 MPa (*SI Appendix*, Fig. S8 *C* and *D*). Untreated leaves showed fluorescence in guard cells in line with research suggesting intermediate basal ABA concentrations in guard cells (45, 47, 49). GFP signals in guard cells were clearly enhanced by exogenous ABA application in the *pRAB18::GFP* transgenic plants (Fig. 4 *C* and *D*). No obvious difference in the guard cell GFP signals was found in the *pRAB18::GFP* transgenic plants grown at 150 or 900 ppm CO_2 for extended periods of time of 24 and 48 h (Fig. 4 *E* and *F*). Overall, these data indicate that elevated CO_2 does not change ABA concentrations in guard cells in response to short-term [CO_2] shifts that cause rapid stomatal responses. Furthermore, long-term exposure to high or low CO_2 does not dramatically alter expression of the *pRAB18::GFP* promoter reporter in guard cells.

Lack of OST1/SnRK2 Protein Kinase Activation in Guard Cells by CO_2 Elevation. OST1/SnRK2.6 is required for stomatal CO_2 responses (27, 28, 36). However, it remains unknown whether the elevated CO_2 signal activates OST1/SnRK2 protein kinases in guard cells. In-gel protein kinase assays were pursued to analyze protein

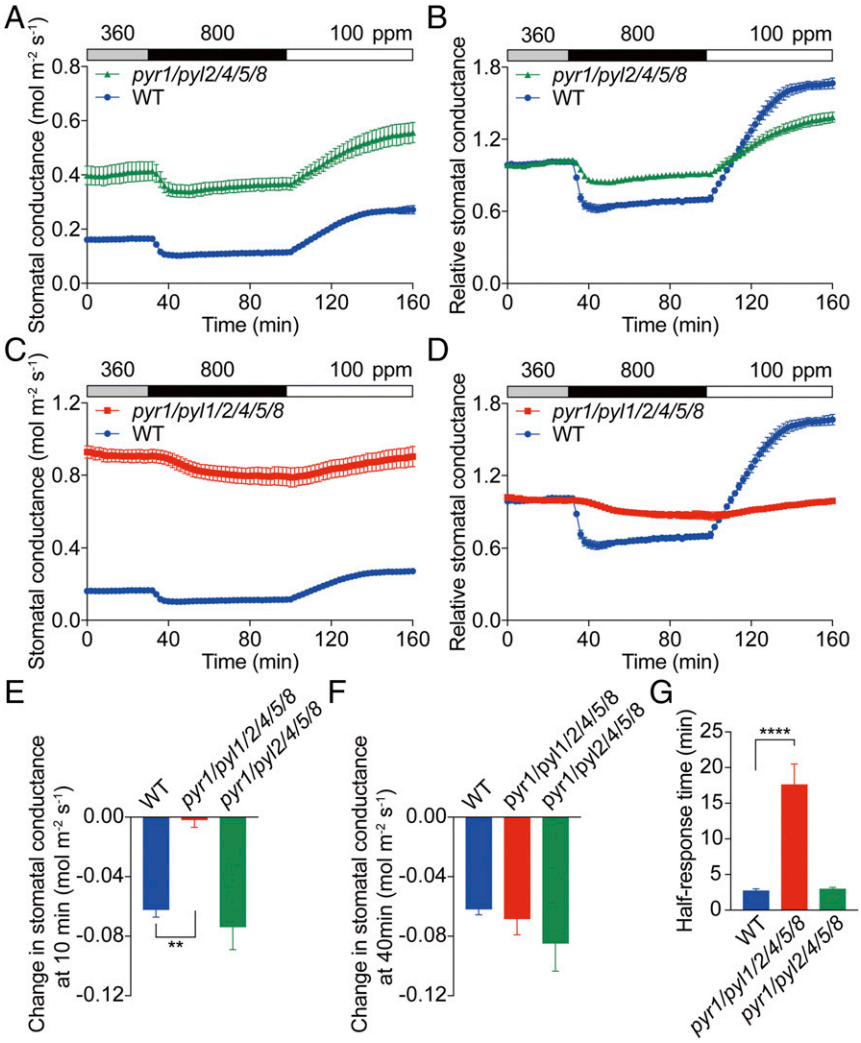

Fig. 3. Stomata of ABA receptor quintuple and hextuple mutants show attenuated stomatal conductance responses to CO_2 concentration changes. Time-resolved stomatal conductance responses to changes in [CO_2] in Col-0 (WT), *pyr1/pyl2/pyl4/pyl5/pyl8* (*rcar3/8/10/11/14*) quintuple mutant (*pyr1/pyl2/4/5/8*), and *pyr1/pyl1/pyl2/pyl4/pyl5/pyl8* (*rcar3/8/10/11/12/14*) hextuple mutant (*pyr1/pyl1/2/4/5/8*) leaves. CO_2 concentrations are shown on top of the data traces in each panel. (*A*) Absolute average stomatal conductances of WT and *pyr1/pyl2/4/5/8* quintuple mutant leaves. (*B*) The corresponding relative stomatal conductance responses shown in *A*. (*C*) Absolute stomatal conductance of WT and *pyr1/pyl1/2/4/5/8* hextuple mutant leaves. (*D*) The corresponding relative stomatal conductance responses shown in *C*. Relative stomatal conductances were calculated by normalizing to the average stomatal conductance at 360 ppm CO_2. Note that data from WT leaves in *A* and *C* are the same because the data were obtained in the same experimental dataset. Absolute reduction in stomatal conductance after switching from 360 to 800 ppm CO_2 for (*E*) 10 min or (*F*) 40 min. (*G*) Average half-response times to 800 ppm CO_2. WT controls are the same because mutants and WT were analyzed in parallel. $n = 5$ plants for WT, $n = 4$ plants for *pyl1/pyl2/4/5/8*, and $n = 4$ plants *pyl1/pyl1/2/4/5/8*. Data represent mean ± SEM. $^{**}P < 0.01$, $^{****}P < 0.0001$ as analyzed by one-way ANOVA followed by a Dunnett's test compared with WT control. Data represent one of three independent sets of experiments showing similar results.

kinase activities in guard cell protoplasts in response to CO_2 concentration changes (Fig. 5). In controls, exposure of guard cell protoplasts to ABA clearly enhanced OST1/SnRK2 protein kinase activity compared with ethanol mock treatments (Fig. 5 and *SI Appendix*, Fig. S9). Unexpectedly, no activation of OST1/SnRK2 protein kinase activity was observed when guard cells were exposed to a high 900 ppm CO_2-equilibrated buffer or to a 13.5 mM $NaHCO_3$ containing buffer for 30 min compared with low 150 ppm CO_2-equilibrated buffer (Fig. 5 and *SI Appendix*, Fig. S9 *A* and *B*). The ABA-responsive kinase activity is most likely due to the OST1/SnRK2.6 protein kinase because the corresponding kinase activity was not detected in *ost1-3* mutant guard cells (Fig. 5*A*) (8, 50). Longer exposure of in-gel kinase ^{32}P signals showed a weak background kinase activity in the range expected for OST1/SnRK2 protein kinases that was, however, enhanced only by ABA but not by 900 ppm CO_2 or $NaHCO_3$ exposure (Fig. 5*B*). These data suggest that CO_2 elevation does not enhance OST1/SnRK2 protein kinase activity in guard cells (see *Discussion*).

To test the possibility that mesophyll (51, 52) cells may be required for guard cell OST1/SnRK2.6 activation in response to CO_2, we treated guard cell protoplasts with CO_2 in the presence of mesophyll cell protoplasts. To distinguish guard cell OST1/SnRK2.6 activity from mesophyll SnRK2 activities, we used a transgenic *ost1-3 Arabidopsis* mutant overexpressing C-terminal HF-tagged OST1/SnRK2.6 (*pUBQ10::OST1-HF/ost1-3*) (53) for guard cell protoplast isolations. ABA is known to activate the OST1-HF isoform (53), which was confirmed here as well (*SI Appendix*, Fig. S10). The presence of Col-0 (WT) mesophyll cell protoplasts showed no effect on the OST1/SnRK2.6-HF activity in guard cells even at a very high CO_2 concentration (*SI Appendix*, Fig. S10).

Elevated CO_2 Activates Guard Cell S-Type Anion Channels Through an ABA-Independent Pathway. Further experiments were pursued to determine whether isolated guard cell protoplasts, as used in the in-gel kinase experiments, respond to leaf CO_2 concentration (Ci) changes in the physiological range (54). Slow-type (S-type) anion channel activation in the plasma membrane of guard cells is a crucial step for both CO_2- and ABA-triggered stomatal closure (24, 27, 28, 31, 55). In previous patch clamp studies of CO_2 responses, relatively high concentrations of CO_2/HCO_3^- have been added to patch clamp pipette solutions that dialyze the cytoplasm of guard cells to study CO_2 regulation of S-type anion channels (27, 28, 30). Here we exposed guard cell protoplasts to more physiological low and elevated extracellular CO_2 concentrations that would result from photosynthesis and respiration in leaves (54). At a low extracellular CO_2 concentration of 115 ppm CO_2, S-type anion channels were not activated, whereas 800 ppm CO_2 in the extracellular buffer caused a clear activation of S-type anion channel currents (Fig. 6).

The CO_2-dependent activation of S-type anion channels was investigated in *nced3/nced5* double mutant and *pyr1/pyl1/pyl2/pyl4/pyl5/pyl8* hextuple mutant guard cells. Similar to WT guard

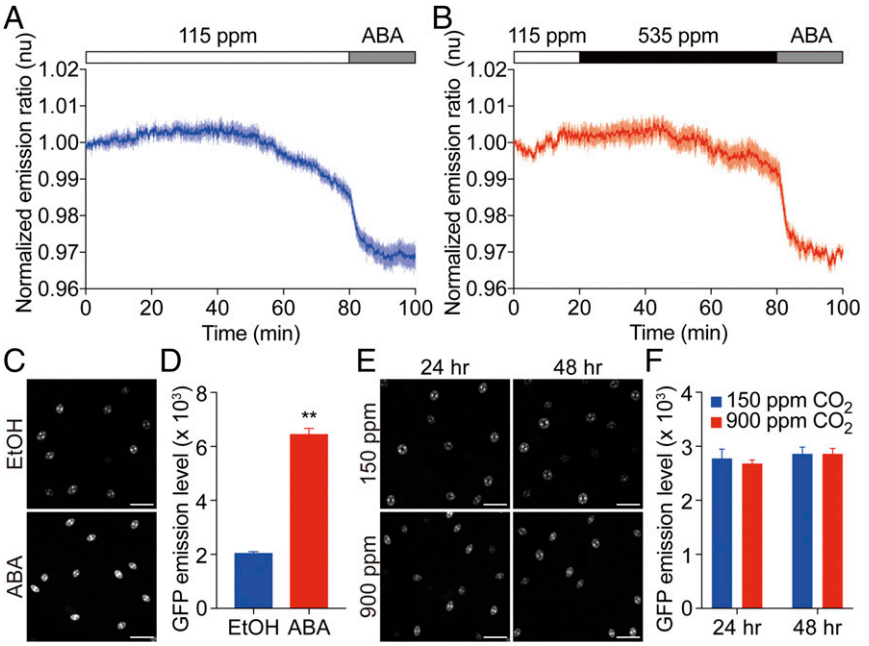

Fig. 4. CO_2 does not rapidly elevate ABA concentration in guard cells. (*A* and *B*) Time-resolved ABAleon2.15 emission ratios in guard cells in response to CO_2 changes and ABA application. Intact leaf epidermes were perfused with buffer containing 115 ppm CO_2 or 535 ppm CO_2 (21) and then switched to a 10 μM ABA containing buffer as indicated. Data in *A* and *B* are averages of normalized emission ratios each from six guard cells. Error bars represent SEM. (*C*) Representative images of *pRAB18::GFP* promoter reporter expression in guard cells in intact leaves in response to ABA or EtOH as control treatment. Rosette leaves of 4-wk-old plants were sprayed with 10 μM ABA or 0.01% EtOH solutions and observed after 24 h. (*D*) Average *pRAB18::GFP* promoter reporter. emission intensity in guard cells under the imposed treatments in *C*. (*E*) Representative images of *pRAB18::GFP* promoter reporter expression in guard cells in intact leaves in response to the indicated CO_2 concentration treatments. Four-week-old plants were grown in a growth chamber at 150 ppm CO_2 for 2 d and then either shifted to 900 ppm CO_2 or maintained at 150 ppm CO_2 for 24 and 48 h. (*F*) Average *pRAB18::GFP* promoter reporter emission intensities in guard cells under the imposed treatments in *E*. GFP intensities were calculated by averaging at least 50 pairs of guard cells in the fourth-youngest leaf of each plant. (Scale bar, 50 μm.) Data represent mean ± SEM. $n = 6$ plants for each treatment. $^{**}P < 0.01$ by Student *t* test.

cells, S-type anion currents in *nced3/nced5* and *pyr1/pyl1/2/4/5/8* guard cells were clearly activated by elevated extracellular CO_2 (800 ppm) compared with low extracellular CO_2 (115 ppm; Fig. 6). These results show that *Arabidopsis* guard cell protoplasts retain responses to physiological CO_2 concentrations. These data provide evidence that WT ABA signal transduction is not required for the rapid CO_2 activation of S-type anion channels in guard cells.

Discussion

Present models for stomatal CO_2 signal transduction in guard cells have been proposed in which (*i*) high CO_2 signaling converges with ABA signaling upstream of or at the level of OST1/SnRK2 protein kinase activation and (*ii*) elevated CO_2 rapidly increases the ABA concentration or ABA signaling in guard cells (see the Introduction). However, direct investigations are needed. In the present study, we addressed the questions how the CO_2- and ABA-signaling pathways converge and whether elevated CO_2 rapidly induces ABA concentration increases in guard cells to trigger stomatal closure. By investigating the stomatal CO_2 responses in ABA signal transduction mutants, we find that ABA signaling amplifies elevated CO_2-induced stomatal closure (Figs. 2 and 3). In addition, the elevated CO_2-triggered stomatal response and the activation of S-type anion channels by extracellular CO_2 elevation in ABA biosynthesis *nced3/nced5* double mutant and ABA receptor *pyr1/pyl1/pyl2/pyl4/pyl5/pyl8* hextuple mutant leaves suggest that ABA signaling is not directly required for this rapid elevated CO_2 response (Figs. 1 and 6 and *SI Appendix*, Fig. S3). Previous research has shown that mutants that disrupt ABA signal transduction cause hyperactivation of plasma membrane proton pumps in guard cells (56). This may contribute to the findings here that ABA receptor hextuple mutant leaves show an attenuated CO_2 response but that CO_2 activation of S-type anion channels is retained. Furthermore, no rapid rise in the ABA concentration of guard cells was observed in response to CO_2 elevation using the ABA FRET-reporter, ABAleon2.15. Moreover, we find that OST1/SnRK2 kinase activities in guard cells are activated by ABA but unexpectedly not by CO_2 elevation (Fig. 5 and *SI Appendix*, Fig. S9). These findings together point to a model for high CO_2-induced stomatal closing mechanisms as discussed further below.

Elevated CO_2 Triggers Rapid Stomatal Closing Through an ABA-Independent Pathway. Recent research has suggested that the elevated [CO_2]-mediated control of stomatal apertures is absent in the *PYR/RCAR* ABA receptor *pyr1/pyl1pyl2/pyl4* (*rcar10/11/12/14*) quadruple mutant and is disrupted in the ABA biosynthesis *nced3/nced5* double mutant (37). In contrast, the present gas exchange results show that stomata in strong ABA biosynthesis *nced3/nced5*, *aba2-1*, and *aba2-11* mutant plants show rapid stomatal closure responses to elevated CO_2 in intact leaves and in intact whole plants. Similar to our observations, stomata in two other ABA biosynthesis mutants, *aba1-1* and *aba3-1*, also responded normally to elevated CO_2 (36, 57). Elevated CO_2-triggered stomatal closure in PYR/RCAR ABA receptor *pyr1/pyl1/pyl2/pyl4* (*rcar10/11/12/14*) quadruple mutant and *pyr1/pyl1/pyl2/pyl4/pyl5/pyl8* (*rcar3/8/10/11/12/14*) hextuple mutant plants is not completely abolished but is clearly slowed. These results agree with previous reports showing that stomata in ABA receptor mutants are still responsive to CO_2 elevation (27, 36). It is unlikely that attenuated elevated CO_2-induced stomatal closure in *pyr1/pyl1/pyl2/pyl4/pyl5/pyl8* (*rcar3/8/10/11/12/14*) hextuple mutant leaves is triggered by additional redundant PYR/RCAR ABA receptor homologs because the stomatal response in *pyr1/pyl1/pyl2/pyl4/pyl5/pyl8* (*rcar3/8/10/11/12/14*)

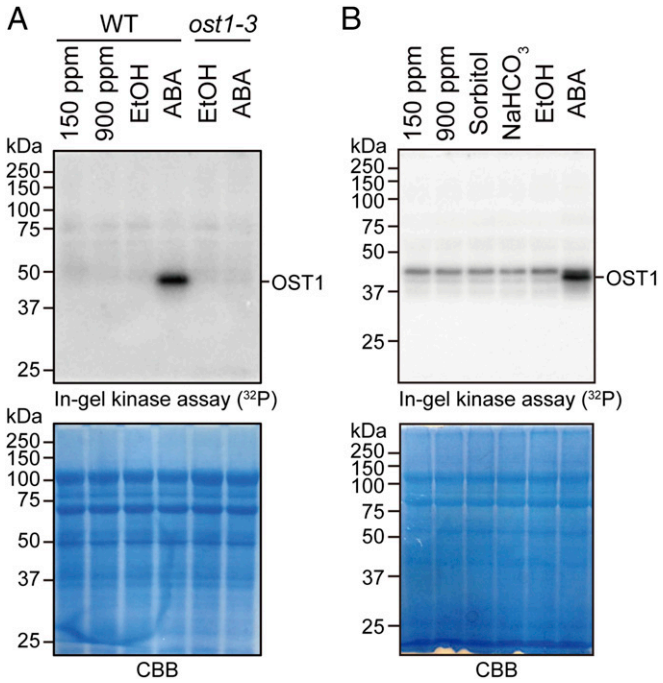

Fig. 5. CO_2 concentration does not affect the OST1/SnRK2 protein kinase activity in guard cells. (*A* and *B*) In-gel kinase assays show OST1/SnRK2 kinase activity in guard cells. Col-0 (WT) or *ost1-3* mutant guard cell protoplasts were incubated in CO_2-equilibrated buffer (150 or 900 ppm CO_2), 10 μM ABA or 13.5 mM $NaHCO_3$ as indicated for 30 min at room temperature; 0.25% EtOH and 27 mM sorbitol were used as controls for ABA and $NaHCO_3$ treatments, respectively. (*B*) Phosphor screen was exposed for 3 d to in-gel kinase gel enabling visualization of basal protein kinase activities at ∼42–45 kDa. CBB staining is shown as a loading control. The presented data are representative results of five independent experiments (see also *SI Appendix*, Fig. S9).

hextuple mutant has been shown to be completely insensitive to ABA (19, 58).

The reasons for differences in the present study and other recent results (37) are not known. Possible explanations could be that steady-state stomatal conductance had been analyzed rather than time-resolved stomatal responses and leaf epidermal peels were used to analyze stomatal apertures in response to exogenous CO_2 concentration changes in a previous study (37). Stomatal aperture responses to CO_2 elevation are attenuated in leaf epidermal peels due to signals from mesophyll cells that are involved in the CO_2 response (51, 52, 59). The present study indicates that long-term stomatal conductance changes to elevated CO_2 depend on ABA synthesis (Fig. 1 *C*, *D*, and *F*), indicating that steady-state stomatal conductance measurements may not always resolve rapid CO_2 signal transduction responses. Conditional effects of *abi1-1* and *abi2-1* on CO_2 control of stomatal closing (60, 61) are consistent with the dominant protein phosphatase 2C nature and activity of these mutations (5, 6, 62) and findings that PP2Cs down-regulate not only SnRK2 kinases but also further downstream targets including the SLAC1 anion channel and transcription factors (35, 63). Furthermore, ABA inhibits the plasma membrane H^+-ATPases, and the dominant ABA signal transduction mutants, *abi1-1* and *abi2-1*, have hyperphosphorylated and hyperactive plasma membrane H^+-ATPases in guard cells (56). This could also contribute to the conditional CO_2 response effects of these dominant PP2C mutant alleles.

Present results show that the activation of S-type anion channels by elevated CO_2 is not abolished in guard cells of *nced3/nced5* double and *pyr1/pyl1/pyl2/pyl4/pyl5/pyl8* hextuple mutants. Together with gas exchange results in ABA biosynthesis mutants, these data provide strong evidence for an ABA-independent pathway for rapid elevated CO_2-induced S-type anion channel activation and stomatal closure. The ABA-independent stomatal closure mediated by elevated CO_2 may in part be explained by a hypothesis in which the SLAC1 anion channel itself might be a CO_2/bicarbonate-responsive protein contributing to CO_2 regulation of S-type anion channels (64). However, SLAC1 regulation by CO_2 is only partial (64), and CO_2 signaling also depends on regulation of upstream protein kinases via an unknown CO_2/HCO_3^- sensing mechanism (22, 29, 30, 65).

Basal ABA as an Amplifier of Rapid CO_2-Induced Stomatal Closure. Under well-watered conditions, leaf ABA content in *aba2-1*, *aba2-11*, and *nced3/nced5* double mutants retained 20–50% of ABA content in WT plants (*SI Appendix*, Fig. S1) (18, 41, 58). We found that stomatal conductances in response to CO_2 elevation in *nced3/nced5* and *aba2-1* mutants gradually increased after rapid CO_2-induced stomatal closing (Fig. 1 *C*, *D*, and *F*). These findings provide evidence that ABA is required to maintain continuous low stomatal conductance at elevated CO_2.

Classical studies showed that ABA enhances CO_2-induced stomatal closing and CO_2 enhances ABA-induced stomatal closing in *Xanthium strumarium* (38, 39), but the basis of this interaction has remained unknown. Plants retain higher basal ABA concentration in guard cells than in mesophyll cells (49). Analyses with ABA FRET-reporters (45, 47) and the ABA-signaling responsive reporter *pRAB18::GFP* (48) (Fig. 4 *C*–*F*) suggest that significant basal levels

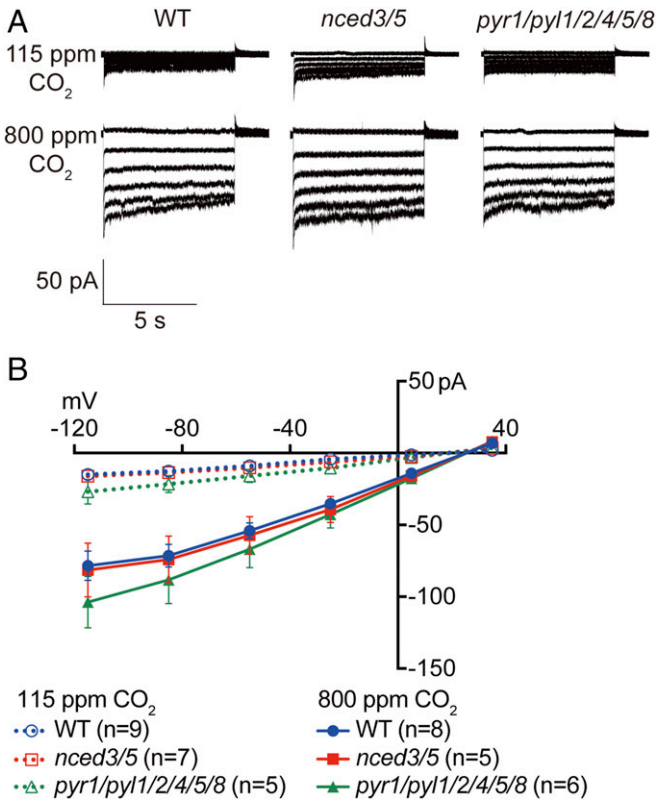

Fig. 6. Elevated CO_2 (800 ppm) activates S-type anion currents in WT, ABA biosynthesis mutant, and ABA receptor mutant guard cell protoplasts. (*A*) Whole-cell recordings of S-type anion currents at the indicated CO_2 concentrations in the bath solution in WT, *nced3/nced5* double mutant (*nced3/5*), and *pyr1/pyl1/pyl2/pyl4/pyl5/pyl8* (*rcar3/8/10/11/12/14*) hextuple mutant (*pyr1/pyl1/2/4/5/8*) guard cells. (*B*) Average current–voltage curves of guard cell S-type anion channel currents recorded in WT, *nced3/5*, and *pyr1/pyl1/2/4/5/8*. Data represent mean ± SEM.

of ABA prevail in guard cells of nonstressed WT plants. Therefore, basal levels of ABA in guard cells may be sufficient to contribute to CO_2 elevation-triggered stomatal closing. Recently, Yamamoto et al. (66) showed that plants expressing truncated SLAC1 isoforms in which the N-, C-, or N- and C-terminal regions were deleted caused disruption of ABA responses but retained a delayed CO_2 induced stomatal closure. The present gas exchange results in ABA receptor mutants suggest that an ABA-dependent pathway amplifies elevated CO_2-induced stomatal closing rather than CO_2 functioning as a direct activator of ABA synthesis and/or of ABA signal transduction.

Genetic studies have shown that the Ser/Thr protein kinase OST1/SnRK2.6 plays critical roles in both ABA- and CO_2-induced stomatal closure (8, 27, 28, 36, 67). ABA-induced stomatal closure is mediated by the activation of the OST1/SnRK2.6 protein kinase in guard cells, which in turn phosphorylates SLAC1 anion channels on N-terminal residues (8, 32–35). Unexpectedly, we find here that OST1/SnRK2 protein kinase activity in guard cells is not measurably enhanced by CO_2 elevation. However, long-term exposures of in-gel kinase assays suggest that a basal activity level of OST1/SnRK2 protein kinase exists in guard cells (Fig. 5*B*) consistent with basal [ABA] in guard cells. Therefore, it is plausible that a basal level of phosphorylation by OST1/SnRK2 protein kinase is required for rapid CO_2-triggered stomatal closing.

In summary, the present study shows that high CO_2-induced stomatal closing is not mediated by a rapid rise in the ABA concentration in guard cells. Furthermore, combined genetic, biochemical, electrophysiological, FRET imaging, and intact leaf and intact whole-plant gas exchange analyses provide strong evidence for a model in which CO_2 and ABA synergistically merge to cause stomatal closing downstream of the OST1/SnRK2.6 protein kinase, but a basal level of OST1/SnRK2 protein kinase activity is required for stomatal closing in response to CO_2 elevation (Fig. 7). The present study further implicates that the stomatal CO_2 response pathway may be in first order independently engineered from drought responses with respect to improving water use efficiency in light of the continuing increase in atmospheric [CO_2].

Materials and Methods

Plant Materials and Growth Conditions. *Arabidopsis thaliana* Columbia-0 (Col-0) ecotype plants were used as wild type. *Arabidopsis* lines in this study were together with *nced3/nced5* double mutant (18), *aba2-1*, *aba2-11* (41), *pyr1/pyl1/pyl2/pyl4* quadruple mutant (5), *pyr1/pyl1/pyl4/pyl5/pyl8* quadruple mutant, *pyr1/pyl2/pyl4/pyl5/pyl8* quintuple mutant, *pyl1/pyl1/pyl2/pyl4/pyl5/pyl8* hextuple mutant (19), *rbohD/rbohF* (43), and *pRAB18::GFP* lines (48). For transgenic *pGC1::ABAleon2.15* plants, a *pGGZ003-pGC1::ABAleon2.15* construct was generated by GreenGate cloning (68) and transformed into Col-0 ecotype by the floral dip method (69). Plants were grown on soil in Percival growth cabinets at a 12/12-h, 21 °C/21 °C day/night cycle, a photosynthetic photon flux density of ∼90 $\mu mol \cdot m^{-2} \cdot s^{-1}$, and 70–80% relative humidity. Plants were watered two times per week to prevent soil drying and drought stress.

For intact whole-plant rosette time-resolved gas exchange analyses, *Arabidopsis* seeds were planted in soil containing 4:3 (volume:volume) peat:vermiculite and grown in pots covered with glass plates as described in Kollist et al. (70). Soil moisture was kept at 80% of maximum water capacity. Plants were grown in growth chambers [AR-66LX and AR-22L (Percival Scientific) and MCA1600 (Snijders Scientific)] at 12/12-h photoperiod, 23/18 °C temperature, 150 $\mu mol \cdot m^{-2} \cdot s^{-1}$ light, and 70% relative humidity. We used 21- to 30-d-old *Arabidopsis* plants in gas exchange experiments.

Time-Resolved Intact CO_2-Dependent Leaf Stomatal Conductance Experiments. Stomatal conductance recordings from intact mature leaves of 5- to 6.5-wk-old plants were conducted starting 1–2 h after growth chamber light onset. A Li-6400XT infrared (IRGA)-based gas exchange analyzer system was used with an integrated 6400-02B LED Light Source (Li-Cor Inc.). The measurement conditions were as described in Hu et al. (26) with some modifications. Leaves were clamped and kept at 360 ppm ambient CO_2, 21 °C, 65–70% relative air humidity, 150 $\mu mol \cdot m^{-2} \cdot s^{-1}$ photon flux density, and 500 $\mu mol \cdot s^{-1}$ flow rate until stomatal conductance stabilized. Flow rates were automatically adjusted to control constant H_2O mole fractions to maintain a stable relative humidity during experiments. For stomatal responses to [CO_2] shifts, stomatal conductance was first measured at 360 ppm ambient CO_2 for 26 or 30 min; then CO_2 concentration was shifted to 800 ppm for the indicated time periods and again changed to 100 ppm for at least 60 min. Following gas exchange experiments, the area of each analyzed leaf was measured for stomatal conductance calculations. Therefore, all calculated stomatal conductances were dependent on the stomatal density, index, and the time-dependent stomatal aperture responses within the chamber. Due to biological variability, the steady-state baseline stomatal conductance can vary in *Arabidopsis* among plants grown at different times of the year (71). Therefore, mutants were always compared with WT plants grown at the same time in each individual experimental set. Gas exchange experiments Figs. 1–3 were repeated in independent experimental sets, and one representative set is shown for each figure panel. The number of leaves averaged in each experimental set is given in the legends of Figs. 1–3. Relative stomatal conductance values were determined by normalization relative to average stomatal conductances at 360 ppm ambient CO_2. Absolute changes of stomatal conductance were calculated by subtracting the last stomatal conductance values at 360 ppm CO_2 from the stomatal conductance values at the indicated time point after 800 ppm CO_2 exposure and in case of slow linear drifts in baseline stomatal conductance, by linear extrapolation of baseline values to the measured time points (e.g., Fig. 3 *E* and *F*). CO_2 response kinetics were approximated by exponential one-phase decays using Graphpad Prism 7.0d software. Data presented are means ± SEM of at least four leaves per genotype per treatment in each individual experimental dataset.

For intact whole-rosette time-resolved stomatal conductance gas exchange analyses, stomatal conductances of plants were recorded with an eight-chamber custom-built temperature-controlled gas exchange device analogous to the one described before (70). Plants were inserted into the measurement cuvettes and allowed to stabilize at standard conditions: ambient CO_2 (∼400 ppm), light 150 $\mu mol \cdot m^{-2} \cdot s^{-1}$, relative air humidity ∼65 ± 3%. Then, CO_2 concentration in the cuvettes was reduced from 400 to 100 ppm for 2 h, thereafter returned to 400 ppm for 2 h and then elevated to 800 ppm for 2 h. Photographs of plants were taken after the experiment, and leaf rosette area was calculated using ImageJ 1.37v (National Institutes of Health). Stomatal conductance for water vapor (gs) was calculated with a custom-written program as described in Kollist et al. (70).

CO_2 Responses of ABA Reporters in Guard Cells. For ABA reporter imaging, 4-wk-old *pGC1::ABAleon2.15* transgenic plants were transferred to a 150-ppm growth chamber for 2 h before experiments. Mature leaves were detached and attached with the abaxial side down to a glass bottom cell culture dish using medical adhesive (Hollister), and upper cell layers were carefully removed with a razor blade resulting in an intact lower leaf epidermis as previously described (21). Intact leaf lower epidermes were incubated in assay buffer (5 mM KCl, 50 μM $CaCl_2$, 10 mM Mes·Tris, pH 5.6) in a

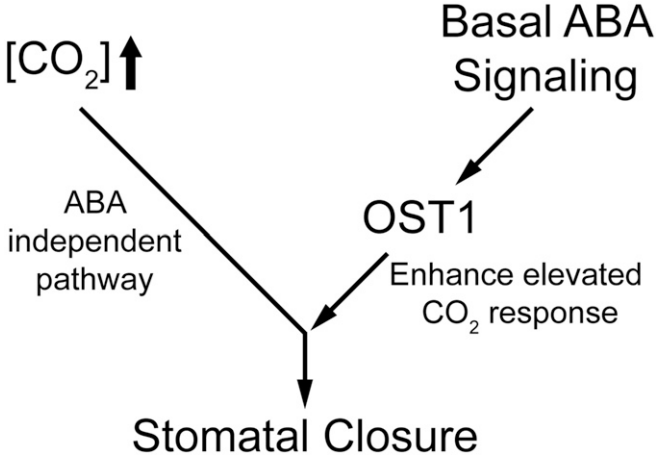

Fig. 7. Schematic diagram of elevated CO_2 and ABA interaction in stomatal closure. Elevated CO_2 and ABA signal transduction merge downstream of OST1/SnRK2.6 to regulate stomatal movements. Elevated CO_2 triggers stomatal closure through an ABA-independent pathway. Basal ABA signal transduction and basal OST1/SnRK2.6 kinase activity are, however, required as amplifier and accelerator of elevated CO_2-triggered stomatal closure.

150-ppm CO_2 growth chamber for an additional hour. Time-resolved ABAleon2.15 emission ratio imaging in guard cells was performed as described in Waadt et al. (45) except using 150-ms exposures to reduce bleaching of fluorescence proteins. During ABAleon2.15 imaging, leaf epidermes were continuously perfused in assay buffer bubbled with CO_2-free air that was passed through soda lime or 800 ppm CO_2 air by a peristaltic pump. By this method, the CO_2 concentration in the CO_2-free and 800 ppm CO_2 equilibrium buffers was determined as 115 and 535 ppm CO_2, respectively, as described previously (21).

For ABA-induced transcriptional reporter imaging, 4-wk-old *pRAB18::GFP* plants (48) were grown in a growth chamber at 150 ppm CO_2 for 2 d and then either shifted to 900 ppm CO_2 or maintained at 150 ppm CO_2 for an additional 24 or 48 h. When indicated, rosette leaves of 4-wk-old *pRAB18::GFP* plants were sprayed with 10 μM (+)-ABA (TCI) or 0.1% EtOH as an ABA solvent control to test the response of *pRAB18::GFP* plants to ABA for 24 h. The fourth-youngest leaf of each individual plant was detached and mounted on a microscope slide with deionized water for imaging. GFP signals were observed and images were captured using a custom-assembled spinning disk confocal microscope system described previously (45). Images were processed and analyzed using Fiji (72).

In-Gel Kinase Assays. *Arabidopsis* guard cell protoplasts (GCPs) were isolated as previously reported (73). We used GCP reaction buffer containing 5 mM Mes-KOH, pH 6.0, 10 mM KCl, 1 mM $CaCl_2$, and 0.4 M mannitol (74). The reaction buffer was incubated overnight in plant growth chambers in which CO_2 concentrations were controlled at 900 or 150 ppm. For $NaHCO_3$ and ABA treatments, GCPs were incubated in the 150-ppm reaction buffer supplemented with 13.5 mM $NaHCO_3$ or 10 μM ABA for 30 min. For CO_2 treatment, GCPs were incubated in the 150- or 900-ppm equilibrated buffer for 30 min. Then, GCPs were harvested by centrifugation at 13,000 × *g* for 1 min and lysed by the addition of SDS/PAGE sample loading buffer. Proteins were separated by SDS/PAGE using gels containing 0.5 mg/mL histone type III-S, and SnRK2 kinase activity was detected by in-gel kinase assays (35, 50).

Patch Clamp Recordings. S-type anion channel activity in guard cells was monitored using the whole-cell patch clamp technique, as previously described (35). One or two rosette leaves were blended in a commercial blender with cold deionized water. Epidermal tissues were collected using a 100-μm nylon mesh and then incubated in 10 mL of a digestion solution that contains 1% (wt/vol) Cellulase R10 (Yakult Pharmaceutical Industry), 0.5% (wt/vol) Macerozyme R10 (Yakult Pharmaceutical Industry), 0.5% (wt/vol) BSA, 0.1% (wt/vol) kanamycin sulfate, 10 mM ascorbic acid, 0.1 mM KCl, 0.1 mM $CaCl_2$, and 500 mM D-mannitol for 16 h at 25 °C at 40 rpm on a shaker. Isolated guard cell protoplasts were collected through a 20-μm nylon mesh and washed three times with a solution containing 0.1 mM KCl, 0.1 mM $CaCl_2$, and 500 mM D-sorbitol (pH 5.6 with KOH). Pipette solutions contained 150 mM CsCl, 5.86 mM $CaCl_2$, 2 mM $MgCl_2$, 6.7 mM EGTA, 5 mM Mg-ATP, and 10 mM Hepes·Tris (pH 7.1). Bath solutions contained 30 mM CsCl, 1 mM $CaCl_2$, 2 mM $MgCl_2$, and 10 mM Mes·Tris (pH 5.6). Osmolarity of the pipette solution and bath solution was adjusted to 485 and 500 mosM with D-sorbitol, respectively. To observe CO_2 responses of S-type anion channels, the bath solution was bubbled with 800 ppm CO_2 or CO_2-free air through soda lime for 30 min before experiments, and the final low CO_2 concentration to which guard cells were exposed after perfusion was determined as described (21). Guard cell protoplasts were preincubated with the CO_2-equilibrated bath solution for 10 min. During experiments, the bath solution was continuously perfused using a peristaltic pump and bubbled with 800 ppm CO_2 or CO_2-free air as described (21). The holding potential was +30 mV, and the voltage was stepped from +35 to −115 mV with −30-mV decrements. Leak currents were not subtracted.

ACKNOWLEDGMENTS. We thank Dr. Annie Marion-Poll for providing *nced3/nced5* double mutant, Dr. Pedro L. Rodriguez for providing higher-order PYR/RCAR ABA receptor mutants, Paulo H. O. Ceciliato for advice on ABA-dependent gas exchange experiments, and Suwayda A. Ali for helping with *pGC1::ABAleon2.15* homozygous plant identification. This research was funded by National Science Foundation Grant MCB-1616236 (to J.I.S.) and in part supported by the National Institutes of Health (GM060396-ES010337 to J.I.S.), a Postdoctoral Research Abroad Program Fellowship sponsored by the Ministry of Science and Technology of Taiwan (104-2917-I-564-008 to P.-K.H.), a Postdoctoral Fellowship for Research Abroad from the Japan Society for the Promotion of Science (to Y.T.), Deutsche Forschungsgemeinschaft Grant WA 3768/1-1 (to R.W.), the Estonian Research Council (IUT2-21 to H.K. and PUT-1133 to E.M.), and the European Regional Development Fund (Centre of Excellence in Molecular Cell Engineering).

1. Shimazaki K, Doi M, Assmann SM, Kinoshita T (2007) Light regulation of stomatal movement. *Annu Rev Plant Biol* 58:219–247.
2. Mott KA (1988) Do stomata respond to CO_2 concentrations other than intercellular? *Plant Physiol* 86:200–203.
3. Kollist H, Nuhkat M, Roelfsema MR (2014) Closing gaps: Linking elements that control stomatal movement. *New Phytol* 203:44–62.
4. Murata Y, Mori IC, Munemasa S (2015) Diverse stomatal signaling and the signal integration mechanism. *Annu Rev Plant Biol* 66:369–392.
5. Park S-Y, et al. (2009) Abscisic acid inhibits type 2C protein phosphatases via the PYR/PYL family of START proteins. *Science* 324:1068–1071.
6. Ma Y, et al. (2009) Regulators of PP2C phosphatase activity function as abscisic acid sensors. *Science* 324:1064–1068.
7. Fujii H, et al. (2009) *In vitro* reconstitution of an abscisic acid signalling pathway. *Nature* 462:660–664.
8. Mustilli AC, Merlot S, Vavasseur A, Fenzi F, Giraudat J (2002) Arabidopsis OST1 protein kinase mediates the regulation of stomatal aperture by abscisic acid and acts upstream of reactive oxygen species production. *Plant Cell* 14:3089–3099.
9. Cutler SR, Rodriguez PL, Finkelstein RR, Abrams SR (2010) Abscisic acid: Emergence of a core signaling network. *Annu Rev Plant Biol* 61:651–679.
10. Raghavendra AS, Gonugunta VK, Christmann A, Grill E (2010) ABA perception and signalling. *Trends Plant Sci* 15:395–401.
11. Joshi-Saha A, Valon C, Leung J (2011) A brand new START: Abscisic acid perception and transduction in the guard cell. *Sci Signal* 4:re4.
12. Finkelstein R (2013) Abscisic acid synthesis and response. *Arabidopsis Book* 11:e0166.
13. Zhu J-K (2016) Abiotic stress signaling and responses in plants. *Cell* 167:313–324.
14. Albert R, et al. (2017) A new discrete dynamic model of ABA-induced stomatal closure predicts key feedback loops. *PLoS Biol* 15:e2003451.
15. Rook F, et al. (2001) Impaired sucrose-induction mutants reveal the modulation of sugar-induced starch biosynthetic gene expression by abscisic acid signalling. *Plant J* 26:421–433.
16. Iuchi S, et al. (2001) Regulation of drought tolerance by gene manipulation of 9-*cis*-epoxycarotenoid dioxygenase, a key enzyme in abscisic acid biosynthesis in *Arabidopsis*. *Plant J* 27:325–333.
17. Nishimura N, et al. (2010) PYR/PYL/RCAR family members are major *in-vivo* ABI1 protein phosphatase 2C-interacting proteins in Arabidopsis. *Plant J* 61:290–299.
18. Frey A, et al. (2012) Epoxycarotenoid cleavage by NCED5 fine-tunes ABA accumulation and affects seed dormancy and drought tolerance with other NCED family members. *Plant J* 70:501–512.
19. Gonzalez-Guzman M, et al. (2012) *Arabidopsis* PYR/PYL/RCAR receptors play a major role in quantitative regulation of stomatal aperture and transcriptional response to abscisic acid. *Plant Cell* 24:2483–2496.
20. Zhao Y, et al. (2016) ABA receptor PYL9 promotes drought resistance and leaf senescence. *Proc Natl Acad Sci USA* 113:1949–1954.
21. Young JJ, et al. (2006) CO_2 signaling in guard cells: Calcium sensitivity response modulation, a Ca^{2+}-independent phase, and CO_2 insensitivity of the *gca2* mutant. *Proc Natl Acad Sci USA* 103:7506–7511.
22. Hashimoto M, et al. (2006) *Arabidopsis* HT1 kinase controls stomatal movements in response to CO_2. *Nat Cell Biol* 8:391–397.
23. Negi J, et al. (2008) CO_2 regulator SLAC1 and its homologues are essential for anion homeostasis in plant cells. *Nature* 452:483–486.
24. Vahisalu T, et al. (2008) SLAC1 is required for plant guard cell S-type anion channel function in stomatal signalling. *Nature* 452:487–491.
25. Meyer S, et al. (2010) AtALMT12 represents an R-type anion channel required for stomatal movement in Arabidopsis guard cells. *Plant J* 63:1054–1062.
26. Hu H, et al. (2010) Carbonic anhydrases are upstream regulators of CO_2-controlled stomatal movements in guard cells. *Nat Cell Biol* 12:87–93, 1–18.
27. Xue S, et al. (2011) Central functions of bicarbonate in S-type anion channel activation and OST1 protein kinase in CO_2 signal transduction in guard cell. *EMBO J* 30:1645–1658.
28. Tian W, et al. (2015) A molecular pathway for CO_2 response in *Arabidopsis* guard cells. *Nat Commun* 6:6057.
29. Hõrak H, et al. (2016) A dominant mutation in the HT1 kinase uncovers roles of MAP kinases and GHR1 in CO_2-induced stomatal closure. *Plant Cell* 28:2493–2509.
30. Jakobson L, et al. (2016) Natural variation in *Arabidopsis* Cvi-0 accession reveals an important role of MPK12 in guard cell CO_2 signaling. *PLoS Biol* 14:e2000322.
31. Schroeder JI, Schmidt C, Sheaffer J (1993) Identification of high-affinity slow anion channel blockers and evidence for stomatal regulation by slow anion channels in guard cells. *Plant Cell* 5:1831–1841.
32. Geiger D, et al. (2009) Activity of guard cell anion channel SLAC1 is controlled by drought-stress signaling kinase-phosphatase pair. *Proc Natl Acad Sci USA* 106:21425–21430.
33. Lee SC, Lan W, Buchanan BB, Luan S (2009) A protein kinase-phosphatase pair interacts with an ion channel to regulate ABA signaling in plant guard cells. *Proc Natl Acad Sci USA* 106:21419–21424.
34. Brandt B, et al. (2012) Reconstitution of abscisic acid activation of SLAC1 anion channel by CPK6 and OST1 kinases and branched ABI1 PP2C phosphatase action. *Proc Natl Acad Sci USA* 109:10593–10598.
35. Brandt B, et al. (2015) Calcium specificity signaling mechanisms in abscisic acid signal transduction in Arabidopsis guard cells. *eLife* 4:e03599.
36. Merilo E, et al. (2013) PYR/RCAR receptors contribute to ozone-, reduced air humidity-, darkness-, and CO_2-induced stomatal regulation. *Plant Physiol* 162:1652–1668.

37. Chater C, et al. (2015) Elevated CO_2-induced responses in stomata require ABA and ABA signaling. *Curr Biol* 25:2709–2716.
38. Raschke K (1975) Simultaneous requirement of carbon dioxide and abscisic acid for stomatal closing in *Xanthium strumarium* L. *Planta* 125:243–259.
39. Raschke K, Pierce M, Popiela CC (1976) Abscisic acid content and stomatal sensitivity to CO_2 in leaves of *Xanthium strumarium* L. after pretreatments in warm and cold growth chambers. *Plant Physiol* 57:115–121.
40. Tanaka Y, Nose T, Jikumaru Y, Kamiya Y (2013) ABA inhibits entry into stomatal-lineage development in Arabidopsis leaves. *Plant J* 74:448–457.
41. González-Guzmán M, et al. (2002) The short-chain alcohol dehydrogenase ABA2 catalyzes the conversion of xanthoxin to abscisic aldehyde. *Plant Cell* 14:1833–1846.
42. Matrosova A, et al. (2015) The HT1 protein kinase is essential for red light-induced stomatal opening and genetically interacts with OST1 in red light and CO_2-induced stomatal movement responses. *New Phytol* 208:1126–1137.
43. Torres MA, Dangl JL, Jones JD (2002) *Arabidopsis* gp91^{phox} homologues *AtrbohD* and *AtrbohF* are required for accumulation of reactive oxygen intermediates in the plant defense response. *Proc Natl Acad Sci USA* 99:517–522.
44. Kwak JM, et al. (2003) NADPH oxidase *AtrbohD* and *AtrbohF* genes function in ROS-dependent ABA signaling in *Arabidopsis*. *EMBO J* 22:2623–2633.
45. Waadt R, et al. (2014) FRET-based reporters for the direct visualization of abscisic acid concentration changes and distribution in Arabidopsis. *eLife* 3:e01739.
46. Yang Y, Costa A, Leonhardt N, Siegel RS, Schroeder JI (2008) Isolation of a strong *Arabidopsis* guard cell promoter and its potential as a research tool. *Plant Methods* 4:6.
47. Waadt R, Hsu PK, Schroeder JI (2015) Abscisic acid and other plant hormones: Methods to visualize distribution and signaling. *BioEssays* 37:1338–1349.
48. Kim TH, et al. (2011) Chemical genetics reveals negative regulation of abscisic acid signaling by a plant immune response pathway. *Curr Biol* 21:990–997.
49. Lahr W, Raschke K (1988) Abscisic-acid contents and concentrations in protoplasts from guard cells and mesophyll cells of*Vicia faba* L. *Planta* 173:528–531.
50. Takahashi Y, Ebisu Y, Shimazaki KI (2017) Reconstitution of abscisic acid signaling from the receptor to DNA via bHLH transcription factors. *Plant Physiol* 174:815–822.
51. Mott KA (2009) Opinion: Stomatal responses to light and CO_2 depend on the mesophyll. *Plant Cell Environ* 32:1479–1486.
52. Fujita T, Noguchi K, Terashima I (2013) Apoplastic mesophyll signals induce rapid stomatal responses to CO_2 in *Commelina communis*. *New Phytol* 199:395–406.
53. Waadt R, et al. (2015) Identification of Open Stomata1-interacting proteins reveals interactions with Sucrose Non-fermenting1-Related Protein Kinases2 and with type 2A protein phosphatases that function in abscisic acid responses. *Plant Physiol* 169: 760–779.
54. Hanstein S, de Beer D, Felle HH (2001) Miniaturised carbon dioxide sensor designed for measurements within plant leaves. *Sens Actuators B Chem* 81:107–114.
55. Raschke K, Shabahang M, Wolf R (2003) The slow and the quick anion conductance in whole guard cells: Their voltage-dependent alternation, and the modulation of their activities by abscisic acid and CO_2. *Planta* 217:639–650.
56. Hayashi M, Inoue S, Takahashi K, Kinoshita T (2011) Immunohistochemical detection of blue light-induced phosphorylation of the plasma membrane H^+-ATPase in stomatal guard cells. *Plant Cell Physiol* 52:1238–1248.
57. Merilo E, Jalakas P, Kollist H, Brosché M (2015) The role of ABA recycling and transporter proteins in rapid stomatal responses to reduced air humidity, elevated CO_2, and exogenous ABA. *Mol Plant* 8:657–659.
58. Merilo E, et al. (2018) Stomatal VPD response: There is more to the story than ABA. *Plant Physiol* 176:851–864.
59. Mott KA, Sibbernsen ED, Shope JC (2008) The role of the mesophyll in stomatal responses to light and CO_2. *Plant Cell Environ* 31:1299–1306.
60. Webb AA, Hetherington AM (1997) Convergence of the abscisic acid, CO_2, and extracellular calcium signal transduction pathways in stomatal guard cells. *Plant Physiol* 114:1557–1560.
61. Leymarie J, Vavasseur A, Lascève G (1998) CO_2 sensing in stomata of *abi1-1* and *abi2-1* mutants of *Arabidopsis thaliana*. *Plant Physiol Biochem* 36:539–543.
62. Finkelstein RR, Somerville CR (1990) Three classes of abscisic acid (ABA)-insensitive mutations of *Arabidopsis* define genes that control overlapping subsets of ABA responses. *Plant Physiol* 94:1172–1179.
63. Lynch T, Erickson BJ, Finkelstein RR (2012) Direct interactions of ABA-insensitive(ABI)-clade protein phosphatase(PP)2Cs with calcium-dependent protein kinases and ABA response element-binding bZIPs may contribute to turning off ABA response. *Plant Mol Biol* 80:647–658.
64. Wang C, et al. (2016) Reconstitution of CO_2 regulation of SLAC1 anion channel and function of CO_2-permeable PIP2;1 aquaporin as CARBONIC ANHYDRASE4 interactor. *Plant Cell* 28:568–582.
65. Hashimoto-Sugimoto M, et al. (2016) Dominant and recessive mutations in the Raf-like kinase *HT1* gene completely disrupt stomatal responses to CO_2 in Arabidopsis. *J Exp Bot* 67:3251–3261.
66. Yamamoto Y, et al. (2016) The transmembrane region of guard cell SLAC1 channels perceives CO_2 signals via an ABA-independent pathway in Arabidopsis. *Plant Cell* 28: 557–567.
67. Yoshida R, et al. (2002) ABA-activated SnRK2 protein kinase is required for dehydration stress signaling in *Arabidopsis*. *Plant Cell Physiol* 43:1473–1483.
68. Lampropoulos A, et al. (2013) GreenGate—A novel, versatile, and efficient cloning system for plant transgenesis. *PLoS One* 8:e83043.
69. Clough SJ, Bent AF (1998) Floral dip: A simplified method for agrobacterium-mediated transformation of *Arabidopsis thaliana*. *Plant J* 16:735–743.
70. Kollist T, et al. (2007) A novel device detects a rapid ozone-induced transient stomatal closure in intact *Arabidopsis* and its absence in *abi2* mutant. *Physiol Plant* 129: 796–803.
71. Azoulay-Shemer T, et al. (2016) Starch biosynthesis in guard cells but not in mesophyll cells is involved in CO_2-induced stomatal closing. *Plant Physiol* 171:788–798.
72. Schindelin J, et al. (2012) Fiji: An open-source platform for biological-image analysis. *Nat Methods* 9:676–682.
73. Ueno K, Kinoshita T, Inoue S, Emi T, Shimazaki K (2005) Biochemical characterization of plasma membrane H^+-ATPase activation in guard cell protoplasts of *Arabidopsis thaliana* in response to blue light. *Plant Cell Physiol* 46:955–963.
74. Takahashi Y, et al. (2013) bHLH transcription factors that facilitate K^+ uptake during stomatal opening are repressed by abscisic acid through phosphorylation. *Sci Signal* 6:ra48.